

See discussions, stats, and author profiles for this publication at: <https://www.researchgate.net/publication/276949065>

Fault location in power networks with mixed feeders using the complex space-phasor and Hilbert–Huang transform

ARTICLE in INTERNATIONAL JOURNAL OF ELECTRICAL POWER & ENERGY SYSTEMS · NOVEMBER 2012

Impact Factor: 3.43 · DOI: 10.1016/j.ijepes.2012.04.012

CITATIONS

13

READS

40

2 AUTHORS:



[Alen Bernadic](#)

Transmission Electricity Company BiH

11 PUBLICATIONS 34 CITATIONS

[SEE PROFILE](#)



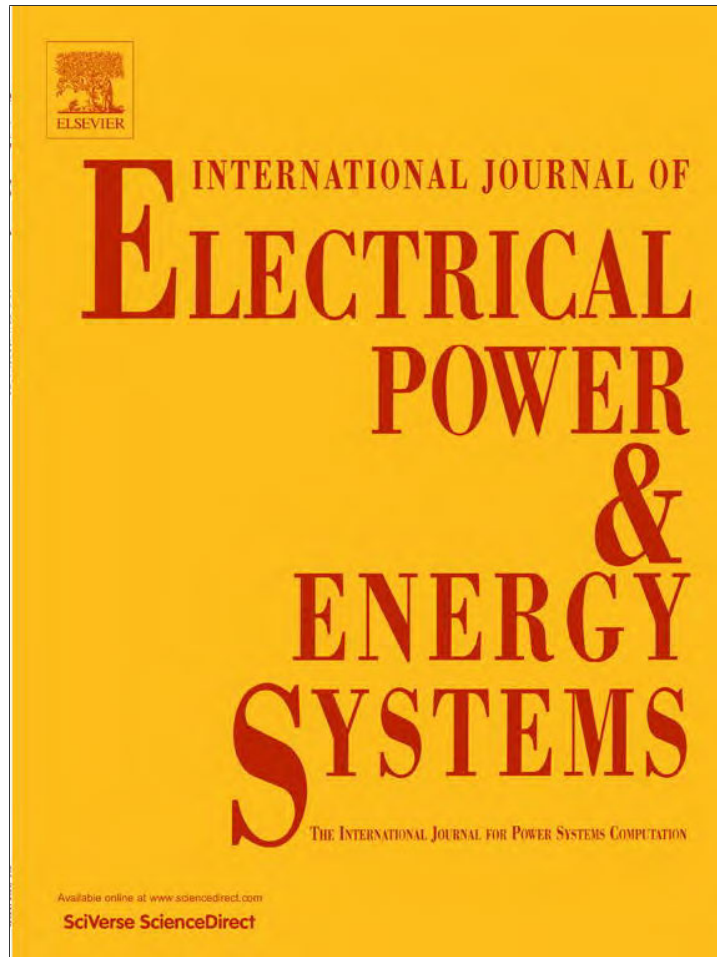
[Zbigniew Leonowicz](#)

Wroclaw University of Technology

105 PUBLICATIONS 763 CITATIONS

[SEE PROFILE](#)

Provided for non-commercial research and education use.
Not for reproduction, distribution or commercial use.



(This is a sample cover image for this issue. The actual cover is not yet available at this time.)

This article appeared in a journal published by Elsevier. The attached copy is furnished to the author for internal non-commercial research and education use, including for instruction at the authors institution and sharing with colleagues.

Other uses, including reproduction and distribution, or selling or licensing copies, or posting to personal, institutional or third party websites are prohibited.

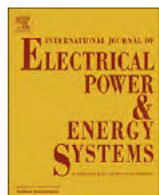
In most cases authors are permitted to post their version of the article (e.g. in Word or Tex form) to their personal website or institutional repository. Authors requiring further information regarding Elsevier's archiving and manuscript policies are encouraged to visit:

<http://www.elsevier.com/copyright>



Contents lists available at SciVerse ScienceDirect

Electrical Power and Energy Systems

journal homepage: www.elsevier.com/locate/ijepes

Fault location in power networks with mixed feeders using the complex space-phasor and Hilbert–Huang transform

Alen Bernadić^a, Zbigniew Leonowicz^{b,*}^aUniversity of Split, Faculty of Electrical Engineering, Mechanical Engineering and Naval Architecture, Croatia^bFaculty of Electrical Engineering, Wroclaw University of Technology, Wroclaw, 50370, Poland

ARTICLE INFO

Article history:

Received 22 October 2011

Received in revised form 7 April 2012

Accepted 9 April 2012

Keywords:

Power distribution faults

Fault location

Transmission line measurements

Power system simulation

ABSTRACT

The paper introduces a practical approach to power system fault location in power networks using advanced fault signal processing. The three phase fault voltages are converted to the vector of absolute values of its complex space phasor. This vector represents fault traveling wave and it is further processed for fault location finding with the Hilbert–Huang transform. The simulation results, including single line to ground faults, faults in mixed feeders and high impedance arcing faults, confirm the accuracy and practical applicability of the proposed approach.

© 2012 Elsevier Ltd. All rights reserved.

1. Introduction

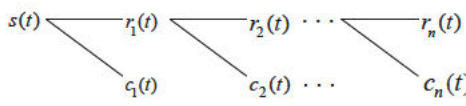
In the majority of power distribution systems of central and southern Europe, electricity distribution feeders (at voltage levels in range from 10 kV to 110 kV) often consist of underground cables and overhead lines (mixed feeders). Furthermore, such mixed feeders may also have different cross sections and very complex topology caused by the growth of the network over the years and increase of power consumption. Responsibility for maintaining the reliability and quality of power delivery lies within the utility companies, who strive to maintain a low Customer Average Interruption Duration Index (CAIDI). Power utilities are encouraged to achieve an acceptable CAIDI level so that a secure and continuous power supply can be maintained. However, interruptions in power supply are sometimes unavoidable due to faults in the power supply system caused by adverse weather conditions and ageing of equipment. Faults need to be identified and located as quickly and accurately as possible so that power restoration can begin immediately. The complexity of modern distribution systems increases the importance of fault location techniques which are considered one of the most interesting research projects in the last years. Conventional techniques such as fault impedance measurements in such difficult conditions as in central and southern Europe represent a problem primarily due to big fault resistance. Measuring instruments and devices for fault location estimation

are usually located in a main distribution substation (i.e. 110/20 kV). Cost reduction of the fault location (avoiding installation of instruments on two or more places in a distribution network) can be achieved with one side current and voltage measurements in combination with computer simulations and calculations and precise planning of the network. Many authors and researchers published various ideas and solutions on this subject. In mathematical sense the leading idea was firstly to decouple measured power system quantities (three phase voltage or currents). In that way, influence of mutual inductance, reactance and capacitance in observed part of power system is lost. As a result, the set of decoupled, physically independent equations are obtained. Those equations in different transformations are usually called modes, and those modes usually become input signals for further processing. Power system fault location issue is improved in last few years with introduction of signal processing methods in power systems studies and analysis. Those methods demand one dimensional signal as input. There exist many possible ways of description of three phase quantities which aim at simplifying the analysis or modeling of electric systems. One of them is the complex space phasor [1].

In recent years many new methods in power system fault location using signal processing methods like Wavelets and Hilbert–Huang transform are published [7,8,19,20]. Novel methods use traveling wave nature of fault transient voltages and currents in power systems. For obtaining of input signal for further processing, the transformations as Karrenbauer and Clarke's transform are often used. As a result of mentioned transformations applied to the three phase signal of measured i.e. busbar voltages, three modes

* Corresponding author.

E-mail addresses: alen.berndic@mocable.ba (A. Bernadić), leonowicz@ieee.org (Z. Leonowicz).

Fig. 1. Decomposition of $S(t)$ signal with EMD.

are obtained (two aerial and one ground mode in Clarke transformation and two line modes and one landline mode in Karrenbauer transformation). Every of those modes are carrier of some physical characteristics of measured three phase quantities. In these procedures only one mode is used as input for processing, which means that a part of physical information from real power system is lost. This is especially important for single phase to ground (SLG) faults, where the ground mode contains important information (usually aerial mode is used for processing in case of Clarke transformation and line mode for processing in case of Karrenbauer transformation of measured quantities).

Although theoretically significant, mentioned novel methods are not always practically applicable. Namely, in the most of published articles, the starting points are known unit inductivity, capacitance and resistance, used in numerical examples. From the assumed parameters the velocity of traveling wave is simply calculated from

$$v = \frac{1}{\sqrt{LC}} \quad (1)$$

and this velocity is taken as input for further processing and fault calculations. With such approach, influence of shunt conductances and series resistances is neglected and speed of traveling wave can strongly influence the accuracy in the practical fault calculations. Furthermore, very high sampling frequency is used in simulations (up to 2 MHz), which is technically often not feasible.

In everyday's practice in TSO's or distribution network operators, precise data about speed of traveling wave is usually unknown. Commonly, data about geometry of overhead lines or underground power cables are known and verified.

In this paper, a practical engineering procedure for fault location calculations will be proposed. These procedures have its roots in complex mathematical methods; however it can be adapted for the practical usage for the transmission or distribution network operators. Firstly we will give a short review of the theoretical assumptions needed for understanding of proposed algorithms. In the next chapters we show calculation examples of the speed of traveling wave and fault location calculations in mixed feeders. The following sections show the validity and accuracy of proposed approach in the case of high impedance arcing faults in mixed feeders.

2. Theoretical background

2.1. Complex space phasor

Complex space phasor is a one dimensional signal which is a carrier of all physical characteristic of measured quantities and is more convenient as preprocessing stage to the state of art signal processing methods like Hilbert Huang transform. In this article we apply the complex space phasor in combination with Hilbert Huang transform which leads to higher accuracy of fault location.

Complex space phasor $f_D = f_\alpha + j f_\beta$ of a three phase system f_R, f_S, f_T is given by [1]:

$$\begin{bmatrix} f_\alpha \\ f_\beta \end{bmatrix} = \sqrt{\frac{2}{3}} \cdot \begin{bmatrix} 1 & \frac{1}{2} & \frac{1}{2} \\ 0 & \sqrt{\frac{3}{2}} & \sqrt{\frac{3}{2}} \end{bmatrix} \cdot \begin{bmatrix} f_R \\ f_S \\ f_T \end{bmatrix} \quad (2)$$

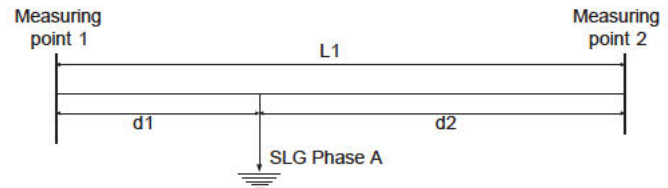


Fig. 2. Illustration of faulted transmission line and measuring points in both ends.

It describes, in addition to the positive sequence component, an existing negative sequence component, including all harmonic and non harmonic frequency components of the signal. In one dimensional signal all physical characteristics and information about measured electrical quantities are comprised. The absolute value of the complex space phasor of measured voltages is processed with Hilbert Huang transformation.

Since the HHT method is described in detail in [9], here we present a short reference only. The main point of HHT is that any complicated data set can be decomposed into a finite and smaller number of components, which is a collection of intrinsic mode functions that represent a generally simple oscillatory mode, not a harmonic function.

2.2. The Hilbert Huang transform

The development of the HHT was motivated by the need to describe nonlinear distorted waves in detail, along with the variations of these signals that naturally occur in nonstationary processes [8]. This method was recently applied in power system studies for analyzing non stationary and nonlinear signals (see, for example, [2–7]). Its application to the transient signals from faulted power system is particularly advantageous. HHT is composed of empirical mode decomposition (EMD) and the Hilbert transform (HT), applied consecutively.

2.3. Empirical mode decomposition (EMD)

The central part of HHT is EMD – a sifting process which results in a signal decomposed into a number of intrinsic modes. The original signal $S(t)$ in a that way, can be expressed as:

$$S(t) = \sum_{i=1}^n c_i(t) + r_n(t) \quad (3)$$

In fact, the EMD is similar to Wavelet decomposition (Fig. 1).

Important is that first IMF $c_1(t)$ contains the highest frequency component of processed signal and this IMF is usually used as input for further processing with Hilbert Transform [9].

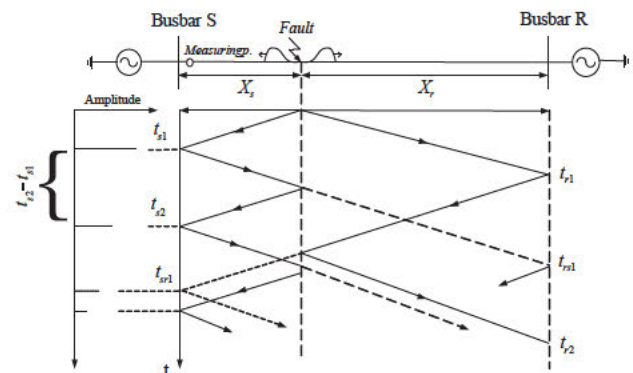


Fig. 3. Lattice diagram – traveling wave phenomenology illustration.

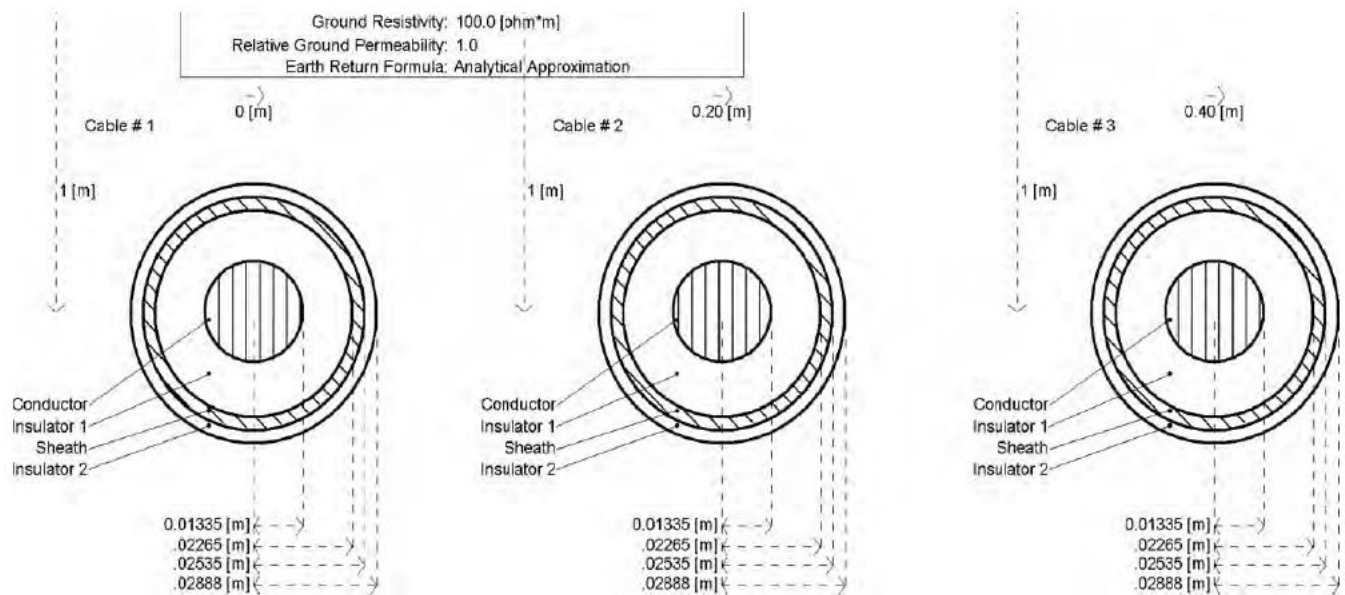


Fig. 4. Underground power 35 kV cable geometry used in simulations.

2.4. Hilbert transform

The Hilbert transform of a real valued time domain signal $X(t)$ is $Y(t)$, such that

$$Y(t) = H[x(t)] = \int_{-\infty}^{\infty} \frac{x(\tau)}{\pi(t - \tau)} d\tau \quad (4)$$

$X(t)$ and $Y(t)$ form an analytical signal:

$$Z(t) = X(t) + Y(t) = A(t)e^{j\theta(t)} \quad (5)$$

with

$$A(t) = \sqrt{X^2(t) + Y^2(t)} \quad (6)$$

and

$$\theta(t) = \tan^{-1} \left[\frac{Y(t)}{X(t)} \right] \quad (7)$$

where $A(t)$ and $\theta(t)$ are instantaneous amplitude and instantaneous phase, respectively. Instantaneous frequency is given by:

$$f(t) = \frac{1}{2\pi} \frac{d\theta(t)}{dt} \quad (8)$$

Calculated instantaneous quantities extract the traveling wave signal of voltages and currents when Hilbert Transform is applied on signal pre processed with EMD.

3. Traveling wave fault location using HHT

After the occurrence of the fault in a power system, a non linear signal of transient traveling wave is generated and runs along the faulted transmission line to both ends of the line. Those traveling waves contain information about fault nature. The fault initial traveling wave has a wide frequency spectrum from DC component to high frequencies. When a traveling wave arrives at the substation busbar, it will change incisively, i.e. traveling wave head will present itself as a sudden change in the time frequency diagram.

As a result of the mutual coupling between adjacent transmission lines or underground cables, the head of fault traveling wave will be deformed which can increase the error of the signal detection procedures. Problem of mutual coupling has been tried to be

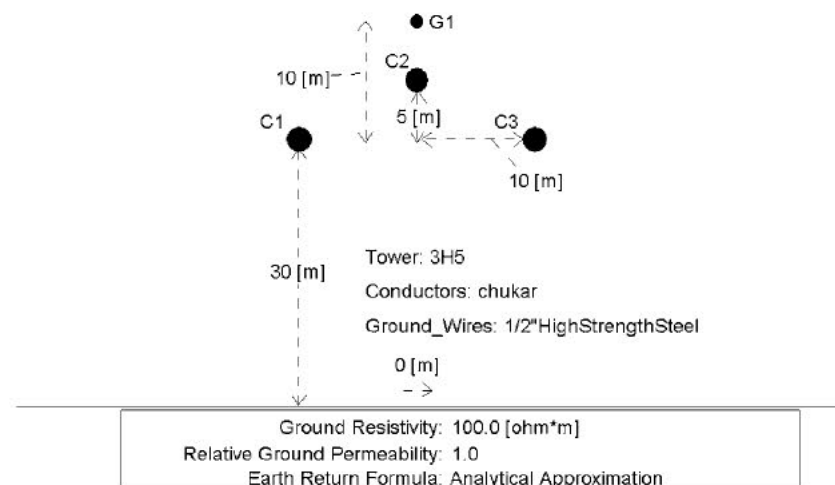


Fig. 5. Overhead line 110 kV geometry used in simulations.

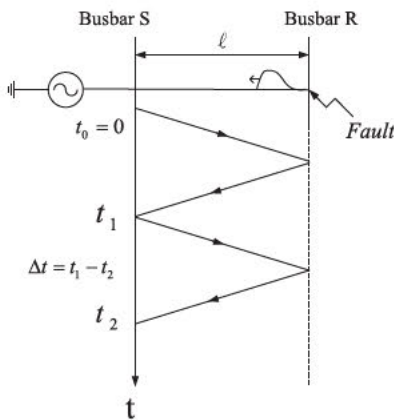


Fig. 6. Traveling wave illustration of experiment for traveling wave speed determination.

solved with decoupling transformations. Karrenbauer and Clarke transformations are the most often used as tool for signal pre processing in recent signal processing analysis of power system fault signals [10].

These transformations decouple measured three phase fault voltages or currents before the analysis using wavelets, HHT or FFT [6,7]. After decoupling, three independent signals modes are obtained. In Karrenbauer transformation those are two line line modes and one landline mode. In Clarke transformation those are two aerial modes and one ground mode. Usually, just one of modes is used for further processing. Furthermore, ground modes are usually omitted in this analysis.

When line line or aerial component mode of traveling wave arrives to the measuring point, the sharp singularity of signal can be detected. Therefore it is possible to determine the fault traveling wave arrival time to the busbars.

Then, the fault signal is decomposed into series of IMF's by empirical mode decomposition (EMD). Researchers showed that the singularity of the fault transient signal is mainly reflected in IMF1 [6], consequently, the IMF1 is selected in this work for further processing and analysis. Omitting of ground modes definitely means that some of important information about the fault is lost, especially if single phase faults to ground are considered. This is the reason why complex space phasor is proposed as a new pre processing method. In such a way, all three measured quantities

i.e. fault voltages are combined into one dimensional signal of complex space phasor. As already mentioned, complex space phasor describe, among others, the negative sequence component which is very important for faults to ground. It was shown in [17] that the use of the complex space phasor allows to achieve better accuracy of fault location in comparison to other decoupling method presented earlier in the literature [6,7,18].

3.1. Fault location calculations

Detailed derivation of formula for fault location is presented in [6,7]. Here we present the reference to the most important relations.

We assume the GPS time synchronization in two substations at both ends of faulted transmission line or underground power cable. Both measuring instruments (fault locators) can measure the time when traveling wave arrives. With L is denoted considered faulted transmission line. In Fig. 2 is presented the considered case.

If we denote the traveling wave arriving times to the both ends with t_1 and t_2 , and with v the speed of traveling wave, the final formula for fault location is [6]:

$$d_1 = \frac{v(t_1 - t_2)}{2} + \frac{L}{2} \quad (9)$$

From (9) it is visible that if we can determine the time when fault traveling waves arrive the two substation busbars, it is possible to calculate fault distance from any of installed fault locators (measuring terminals).

3.2. Traveling wave theory

In terms of transients, underground cables and overhead lines show very different characteristics. The major difference is their shunt capacitance. Due to smaller distances between conductors and different insulation materials, underground cables have usually a much higher shunt capacitance compared with overhead lines of the same rating and voltage level. Also the series inductance differs; normally it is slightly lower for cables. The traveling wave (TW) propagation velocity depends on both parameters, and is usually lower for cables than for overhead lines. Junction point of overhead lines and underground cables is also point of discontinuity in terms of physical characteristics.

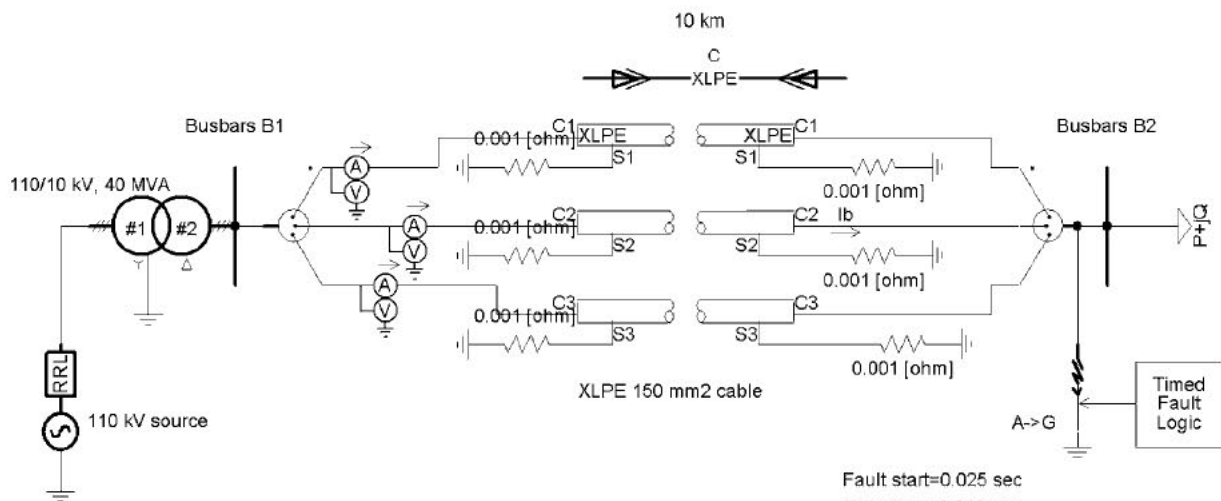


Fig. 7. Simulation setup in EMTDC used for calculating a speed of complex space-phaser along XLPE underground power cable.

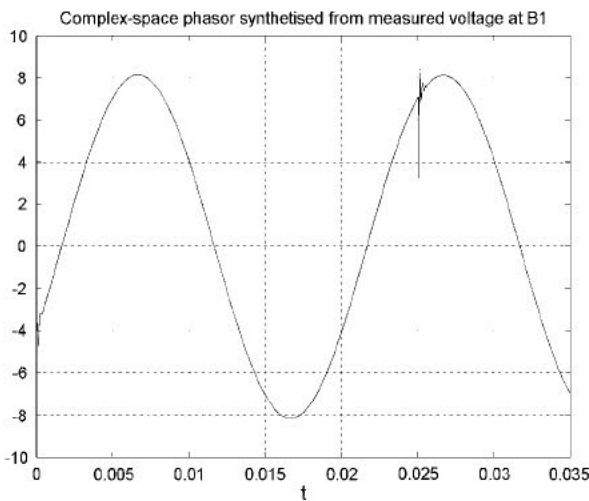


Fig. 8. Signal of complex space-phasor values (synthesized from measured voltages at B1).

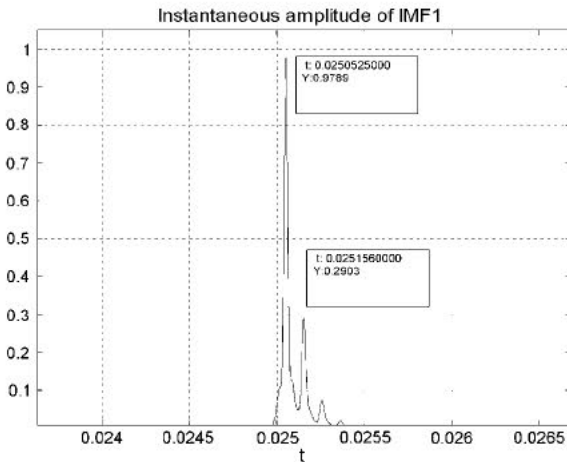


Fig. 9. Instantaneous amplitude of IMF1 component of complex space-phasor synthesized from measured voltages at B1.

According to TW theory, any disturbance or a sudden change in an overhead transmission line or underground cable will generate both forward and backward traveling wave signals propagating away from the disturbance point towards both busbars. The initial values of these waves are dependent on several factors such as fault position, fault path resistance, fault inception angle [3,20,21] and type of fault. Further, these signals will be reflected and refracted at the points of discontinuity, i.e. fault point, busbars or junction of underground cable and overhead line, until they are attenuated to a negligible value. The basic principle of this method can be well explained using Bewley's lattice diagram for fault at first half of transmission line from measuring point at busbar S, as illustrated in Fig. 2. When a wave arrives at a discontinuity, such as an open circuit or a short circuit, or at a point on the line where the characteristic impedance changes, a part of the energy is let through and a part of the energy is reflected and travels back. Fig. 3 shows the case in which an overhead transmission line is short circuited at the first half of its length.

3.3. Geometry of overhead lines or power underground cable; traveling wave nature of complex space phasor

Contemporary simulation programs are able to calculate physical parameters of overhead transmission lines or underground

cables precisely for given conductors' geometry and material characteristics (Fig. 4 and 5); these parameters are known.

In Fig. 5 an overhead line model is given which is used in this work as an example. Cross section of considered overhead line is 150 mm², and transposed and balanced line is assumed.

4. Speed of the complex space-phasor traveling wave along overhead line and underground power cable

Complex space phasor is chosen for traveling wave because of its quoted physical properties. It will be shown that complex space phasor has all traveling wave characteristics including the most important one – the correct wave speed. Speed of traveling wave can be determined from a simple simulation, as illustrated in Fig. 6.

$$v = \frac{2 \cdot \ell_{\text{line}}}{\Delta t} \quad (10)$$

where ℓ_{line} is length of the overhead line or underground power cable, Δt is time between two peaks on wave shapes determined by measuring instruments. Methods for secure determination of traveling (voltages or currents) wave peaks and their corresponding occurrence times must be chosen.

4.1. Speed of complex space phasor along underground power cable

The verification of theoretical assumptions involves the determination of the speed of complex space phasor along underground power cable with insulation. For this purpose a simple simulation is shown. The most used insulating material for underground power cables is the Cross Linked Polyethylene (XLPE). It is quoted [6] that the most important problem is to clearly distinguish singularity points in traveling wave to apply relation (10). For that purpose, three phase fault voltages will be converted into signal of absolute values of complex space phasor and processed with Hilbert Huang transform in order to find exact time and non doubtful singularity points. A simple power system configuration is taken for illustration of complex space phasor speed determination. Strong 110 kV network equivalent is simulated with Thevenin's source taken from standard EMTDC library. Middle voltage (10 kV) network is connected over grid transformer 110/10 kV, 40 MVA, Y Δ with just one underground power XLPE cable of 150 mm², and 10 km length is connected to the symmetrical load. At the end of cable with given geometry a single line to ground fault in phase A is simulated. Fault voltages are recorded by measuring instruments with 2 MHz frequency in the main substation at 10 kV busbars.

Entire time of observed transient phenomenon is $t = 0.035$ s, and single line to earth fault is simulated in phase A at $t_0 = 0.025$ s. Simulation setup is illustrated in Fig. 7.

Single phase to ground fault is simulated at the end of XLPE power cable of given geometry. Measured voltages can be recorded on workspace and prepared for further processing. As the first step we converted recorded measured three phase fault voltages from busbar B1 into signal of absolute values of their complex space phasor (Fig. 8).

In this work, the absolute values of complex space phasor are chosen for pre processing of measured three phase fault voltages. In Fig. 9 the absolute value of complex space phasor synthesized from measuring fault voltages at busbar B1 is presented (fault inception $t_0 = 0.025$ s). In the moment of fault inception, singularity in complex space phasor will be detected on measuring instruments installed at main substation, at 10 kV busbars B1. Traveling wave will be reflected to the busbars B1 as on Fig. 6. Then, IMF components of fault traveling wave will be extracted by means of empirical mode decomposition (EMD) (Fig. 9).

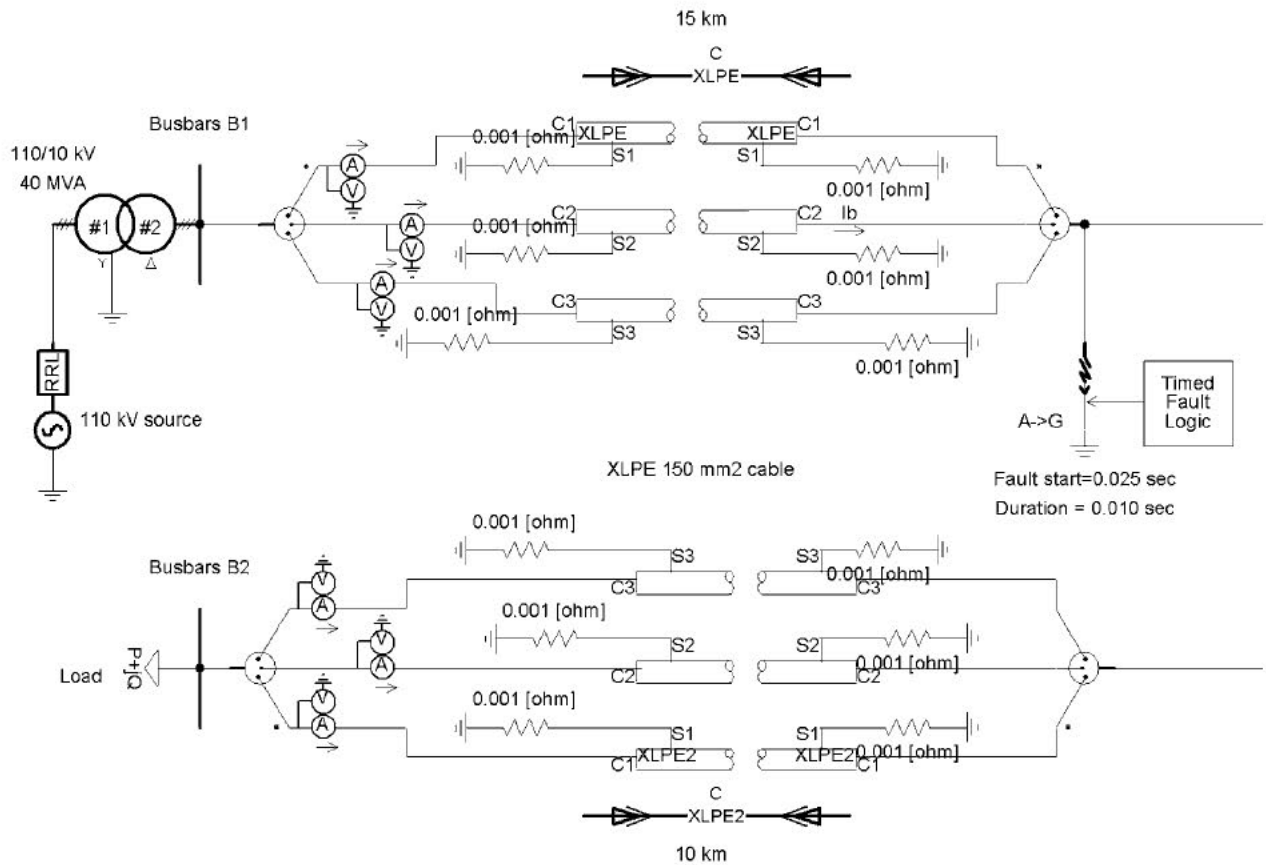


Fig. 10. Simulation setup in EMTDC used for calculating a fault location at XLPE underground power cable. Fault is simulated at 15th kilometer from B1.

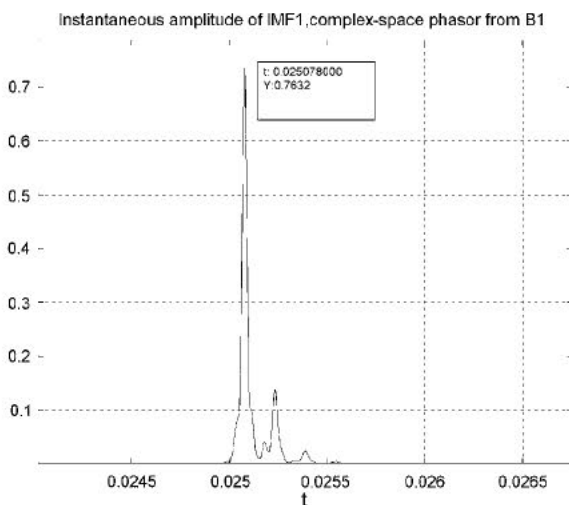


Fig. 11. Instantaneous amplitude of IMF1 component of complex space-phasor synthesized from measured voltages at B1.

The relation (10) can be used for calculating and the velocity of complex space traveling wave along selected XLPE power cable. Consequently, the speed of

$$v = 1.93236 \times 10^8 \text{ m/s} \quad (11)$$

is obtained.

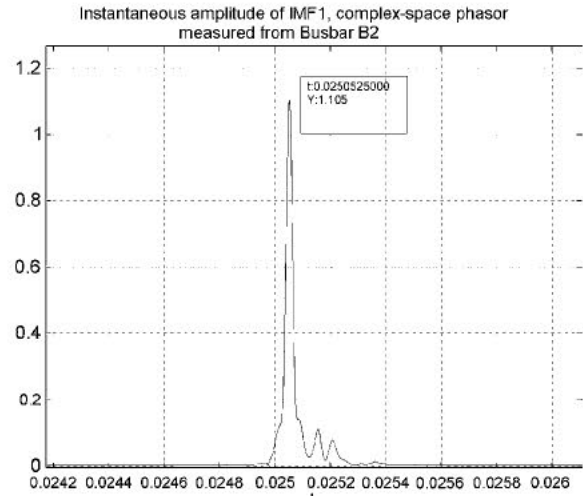


Fig. 12. Instantaneous amplitude of IMF1 component of complex space-phasor synthesized from measured voltages at B2.

4.2. Example: Single line to ground fault at XLPE underground cable; HHT procedure for fault calculations from known speed of complex space phasor

The effect of the traveling waves is more harmful if the system is connected by cables rather than by overhead lines. The reason is that the characteristic impedance of cables ($<40 \Omega$) is lower than the characteristic impedance of overhead lines ($300-400 \Omega$) and, the lower the surge impedance the higher the time derivatives of the voltage generated in the terminals of the equipment.

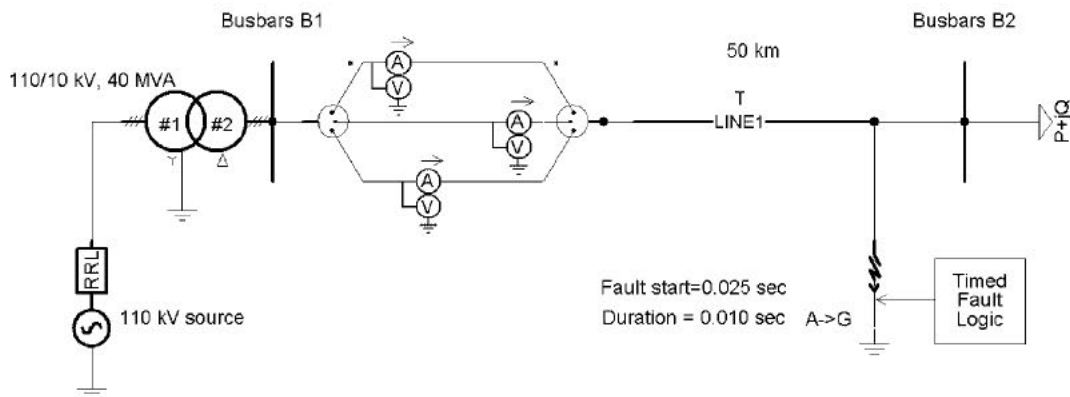


Fig. 13. Simulation setup in EMTDC used for calculating a speed of complex space-phasor along overhead line.

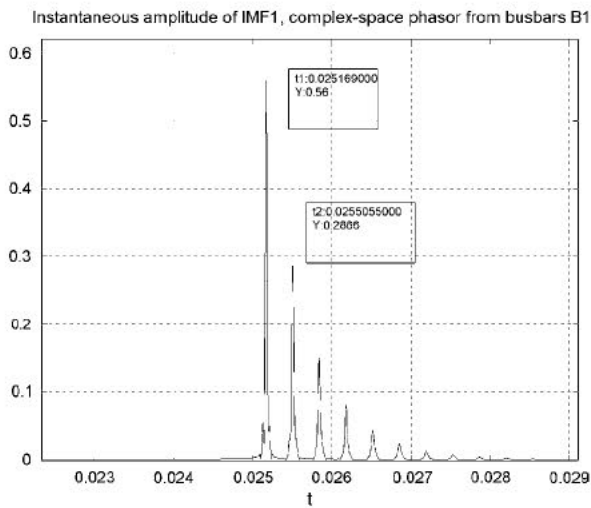


Fig. 14. Instantaneous amplitude of IMF1 component of complex space-phasor synthesized from measured voltages at B1 – case for determining speed of complex space-phasor along overhead line.

Practical cases in everyday's work of network operators are, in most cases, single line to ground faults. Statistically, those faults are the most frequent by occurrences. As a proof that speed of complex space phasor is correct physical quantity the case illustrated with Fig. 10 will be processed for fault location at XLPE cable.

At the moment of fault inception, singularity in complex space phasor will be detected on fault locators installed on both ends. IMF components of fault traveling wave will be extracted by means of empirical mode decomposition (EMD). Earlier works [6–8] showed that volatility and singularity of the transient signal is mainly reflected in IMF1 component. In this work the IMF1 component is selected for further processing. With Hilbert Huang transform we extract instantaneous amplitude and instantaneous frequency of processed signal and fault location can be determined from (9). In [6] is shown that instantaneous amplitude is sufficient for fault location calculation.

4.3. Calculation procedure and results

Single line to ground fault is simulated at 15th kilometer of faulted underground XLPE cable measured from busbar one (B1), with fault resistance $R_{\text{ground}} = 150 \Omega$ (Fig. 10).

Figs. 11 and 12 represent the instantaneous amplitude of traveling wave which are recorded at both ends at fault locators.

Before the fault occurrence, the instantaneous amplitude is flat. When the head of traveling wave reaches the measuring instrument, the instantaneous amplitude clearly change, i.e. singularity can be easily detected (Figs. 12 and 13). From the first singularity point the traveling wave arriving time is computed. From obtained measurements the distance of $d = 14.9637$ km is calculated using relation (9) and value (11). The error is 36.23 m.

4.4. Speed of complex space phasor along overhead line

In the similar way we can calculate speed of complex space phasor along the overhead line. For this simulation the overhead line with geometry given in Fig. 5 is used. Simulation configuration is given in Fig. 13.

At the moment of fault inception, singularity in complex space phasor will be detected by measuring instruments installed at main substation, at 10 kV busbars B1. Traveling wave will be reflected to the busbars B1 as on Fig. 6. Then, IMF components of fault traveling wave will be extracted by means of empirical mode decomposition (EMD) (Fig. 14).

Relation (10) can be used for calculating and the velocity of complex space traveling wave along selected overhead line.

The speed

$$v = 2.9717 \times 10^8 \text{ m/s} \quad (12)$$

is obtained.

4.5. Example: Single line to ground fault at mixed feeder with OHL and XLPE; HHT procedure for fault calculations using known speed of complex space phasor

In majority of power distribution systems of central and southern Europe, electricity distribution feeders (voltage levels in range from 10 kV to 110 kV) often consist of underground cables and overhead lines (mixed feeders). Furthermore, such mixed feeders also may have different cross sections and very complex topology caused by growth of electricity consumption and network rebuilds. That is the reason why it is important to find a way for effective determining of the fault location in such a feeders. Furthermore, in practical cases, it is often enough just to determine which part of the mixed feeder is affected by the fault.

As a starting point, we assume a mixed feeder consisting of 10 km XLPE underground cable and 20 km overhead line as illustrated in Fig. 15. Single line to ground fault is simulated at discontinuity point, i.e. the junction point of XLPE cable and overhead lines, with geometry given at Figs. 4 and 5.

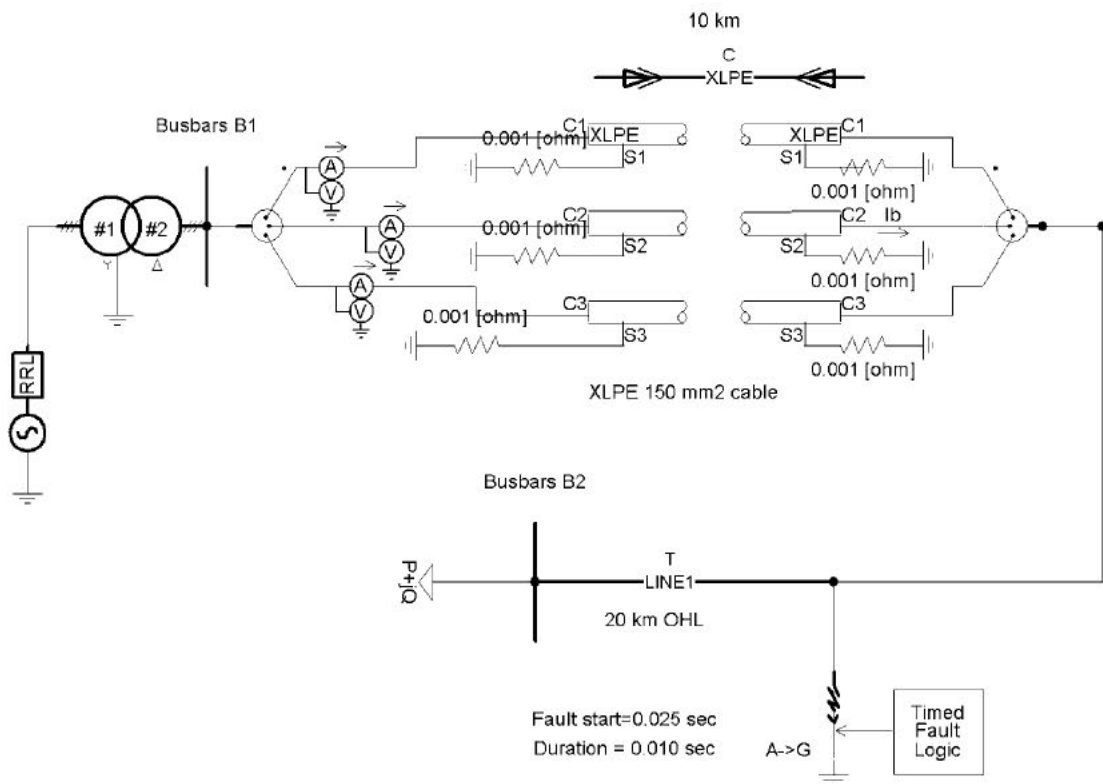


Fig. 15. Simulation setup in EMTDC used for determining characteristic singularity points of complex space-phasor in a case of fault in singularity point (junction of overhead line and XLPE underground cable).

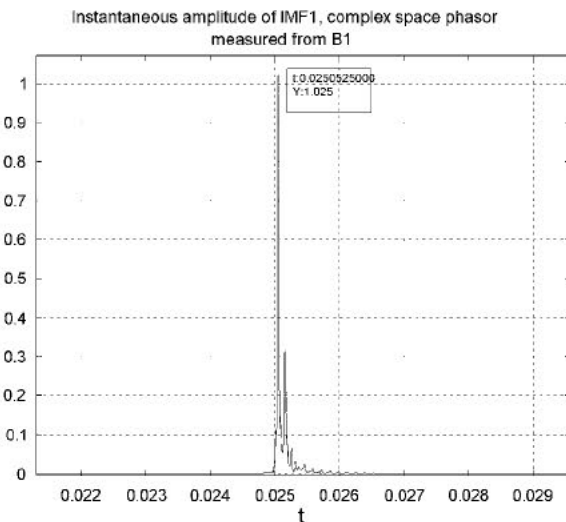


Fig. 16. Instantaneous amplitude of IMF1 component of complex space-phasor synthesized from measured voltages at B1.

Considering all assumptions presented before, it is important to record traveling wave behavior of complex space phasor for this fault as a reference. The EMD and HHT procedure is conducted as in the case of homogeneous feeders.

Those values (presented in Fig. 16 and 17) for characteristic fault at junction point of XLPE and overhead lines will be referential points for fault location considerations at mixed feeders presented in next sections. Basic idea is to compare singularities obtained via EMD and HHT for different cases, considering all the theory already presented and values for traveling wave speed of complex space phasor along homogeneous feeders.

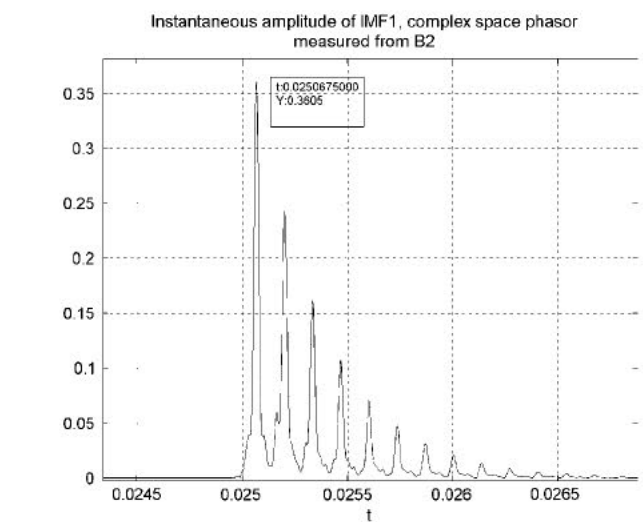


Fig. 17. Instantaneous amplitude of IMF1 component of complex space-phasor synthesized from measured voltages at B2.

4.6. Example: Single line to ground fault at mixed feeder with OHL and XLPE; HHT procedure for fault calculations

As first case we will consider fault at proposed mixed feeder configuration, with single line to ground fault at 5th kilometer of XLPE underground cable (Fig. 18).

It is important to show relations between singularity points of IMF1's for real fault case and reference fault case (simulated fault at junction point). Comparing IMF's singularity points obtained from complex space phasor from both feeders ends a useful relation for fault location determination can be derived. At Fig. 19 is

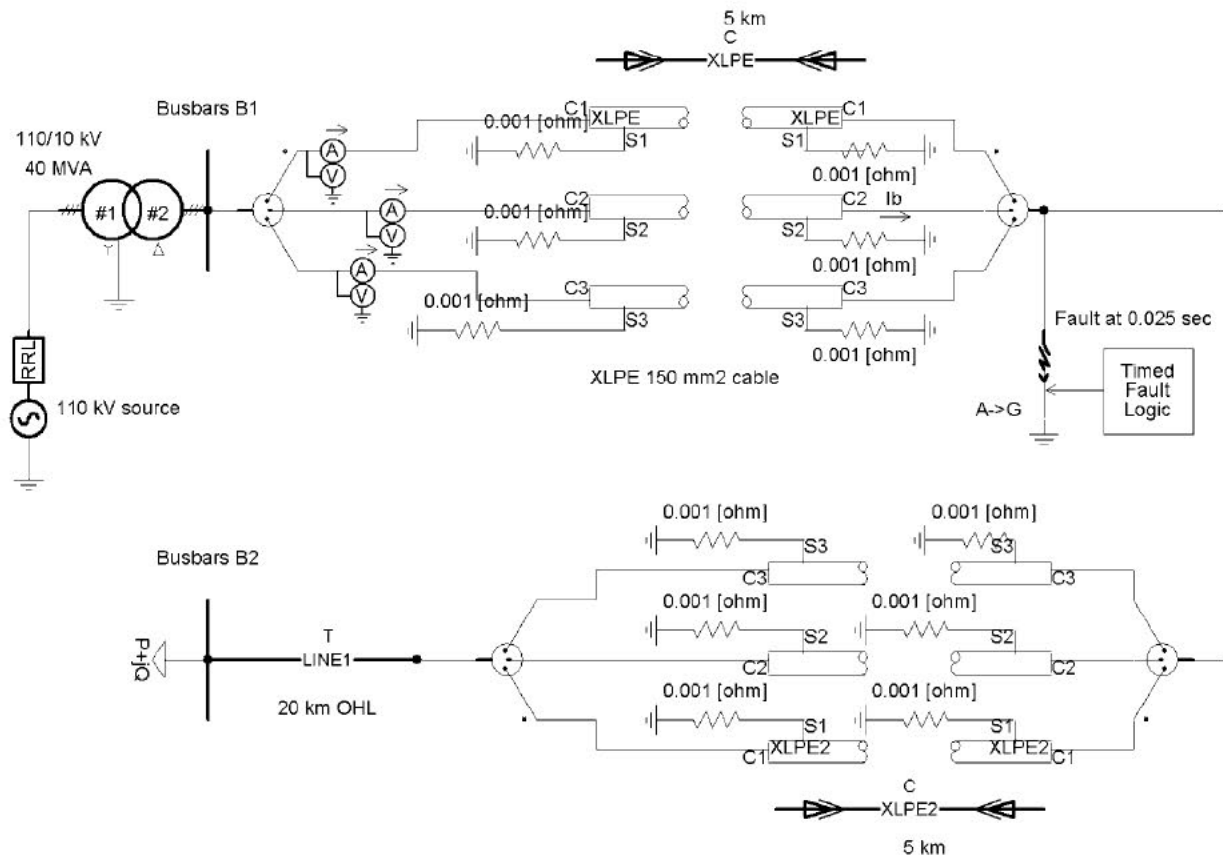


Fig. 18. Simulation setup in EMTDC used for determining complex space-phasor in a case of fault on 5th kilometer of XLPE cable.

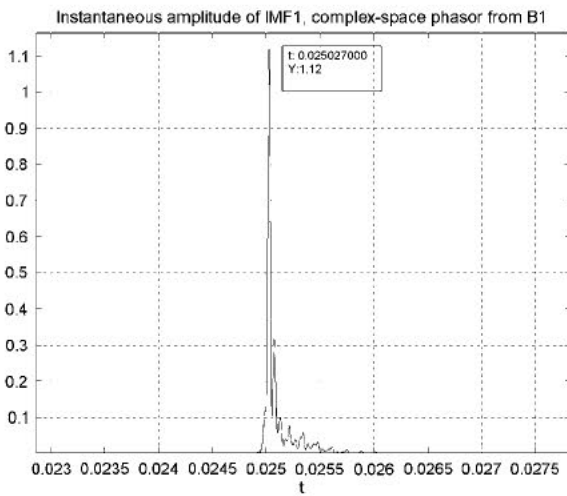


Fig. 19. Instantaneous amplitude of IMF1 component of complex space-phasor synthesized from measured voltages at B1.

shown the IMF's of the complex space phasor synthesized from busbar B1 measuring voltages, for fault case from Fig. 18, i.e. single line to ground fault at 5th kilometer of XLPE cable.

Comparing it with reference case (the case with single line to ground fault, Fig. 16, (time of fault inception $t = 0.0250525$) we remark that singularity point in instantaneous amplitude for fault at 5th kilometer of XLPE underground cable shows up earlier ($t = 0.025027$) comparing to case with fault at junction point of XLPE and OHL. It means that complex space phasor did not tra-

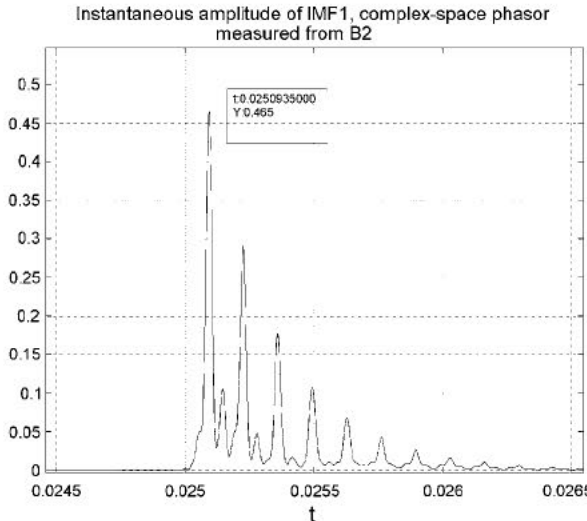


Fig. 20. Instantaneous amplitude of IMF1 component of complex space-phasor synthesized from measured voltages at B2.

verse all length of XLPE cable. The first conclusion from traveling wave characteristics of complex space phasor is that fault is inception somewhere at underground XLPE power cable.

Furthermore, from difference of singularity occurrence times it can be calculated and correct fault location, again using the reference case from Fig. 18 (fault at junction point). Time difference is:

$$dt \quad 0.0250525 \quad 0.025027 \quad 0.0000255 \text{ s} \quad (13)$$

If we multiply (13) with the speed of complex space phasor along XLPE (11), we obtain the fault location at the distance of 4927.5 m, which is the distance from fault location to the junction point of XLPE and overhead line. It follows that the fault location is at $d = 5072.5$ m (the error is 72.5 m).

Conversely, taken the instantaneous amplitudes of IMF's from complex space phasor synthesized from busbars B2 (another feeder end) the fault location with satisfactory correctness can be calculated, as well (Fig. 20).

The first important fact is the time of first singularity occurrence of instantaneous amplitude IMF's of complex space phasor which is greater than in reference case (Fig. 17). It means that the traveling wave traversed more than length of overhead line and the fault should be found on XLPE power cable. Furthermore, from its time differences we obtain:

$$dt = 0.0250935 \quad 0.0250675 \quad 0.000026 \text{ s} \quad (14)$$

Multiplying (14) with the speed of complex space phasor along XLPE (11), we obtain the distance of 5024.2 m, which corresponds to the distance from the junction point to the fault point. The result of fault location is the sum of the length of overhead line and 5024.154 m, so the error is 24.2 m.

Using the same methodology, using (11) and (12) along with time differences of singularity occurrences, the results for fault calculation at mixed feeder are shown in Table I.

5. High impedance fault location

The procedure using complex space phasor and HHT is also applicable for fault location calculation in case of the worst scenario for protection relays, equipment and power system diagnostics in general – high impedance fault (HIF) occurrence.

Detection of high impedance arcing faults (HIF) presents still important and unsolved protection problem, especially in distribution networks. Location of the HIF fault of the feeder with arcing faults is not trivial since the ground fault current in MV networks is very low, often below load current of the feeder.

Several approaches for the detection of HIFs may be found in the literature, as, for example, presented in [14,16].

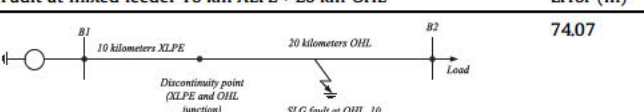
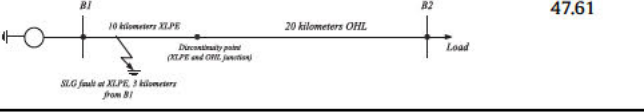
In this chapter we test the validity of proposed approach in various cases with HIF arcing faults.

5.1. Arc model

The high impedance ground fault model applied in the simulation experiments was developed basing on research and considerations presented in [11–13] but also new features were included into the model implementation. To obtain dynamic features of the ground fault nonlinear impedance the digital arc model described in [11] was adopted. This model is based on the Hochrainer arc description, derived under assumption of an energy balance in the arc and is described by the following differential equation [14]:

Table I

Fault cases for considered mixed feeder.

Fault at mixed feeder 10 km XLPE + 20 km OHL	Error (m)
	74.07
	47.61

$$\frac{dg}{dt} = \frac{1}{\tau}(G - g) \quad (15)$$

where g – time varying arc inductance, G – stationary arc inductance and τ – the time constant.

The stationary arc conductance follows as:

$$G = \frac{|i|}{(u_0 + R|i|)l} \quad (16)$$

where i – arc current, u_0 – constant voltage per arc length unit, R – resistance per arc length unit, l – arc length.

The arc parameters chosen in the following simulations were:

$$l = 0.15 \text{ m}, \quad \tau = 2.5 \times 10^{-5} \text{ s}, \quad R = 10^3 \Omega/\text{m}, \quad u_0 = 1500 \text{ V/m}$$

The developed arc model was implemented using the PSCAD (EMTDC) [15] simulation package (Fig. 23). Diodes and polarizing voltages were used to shift arc ignition moments. The arc model consists of the linear resistor (representing the ground path resistance), the nonlinear time varying resistor (representing the dynamic arc) as well as DC and AC sources. The sources ensure asymmetry of the arc current and voltage (DC sources) and variable arc ignition and quenching point (AC sources).

The simulation results of the arc current (Fig. 21) correspond to the experimental results presented in [14]. The high impedance model was connected to the modeled MV network at points of fault inception.

5.2. High impedance fault at feeder with OHL; HHT procedure for fault calculations

HIF fault is simulated at 5th kilometer of faulted overhead line measured from busbar B1, using above described HIF simulation component implemented in external Fortran 77 procedure (Figs. 22 and 23).

At the moment of fault inception, singularity in complex space phasor will be detected by measuring instruments installed at

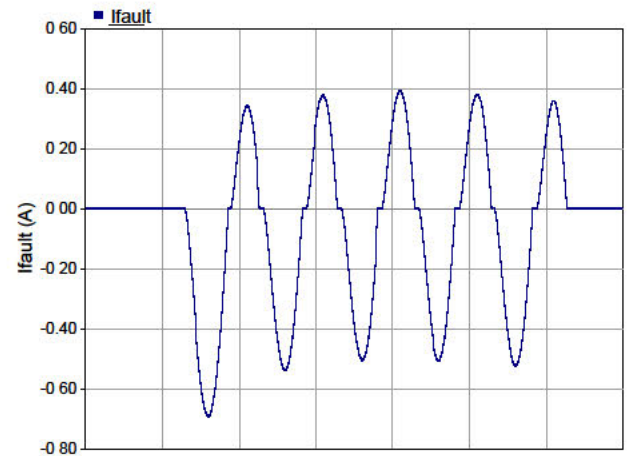


Fig. 21. Waveform of the arc current.

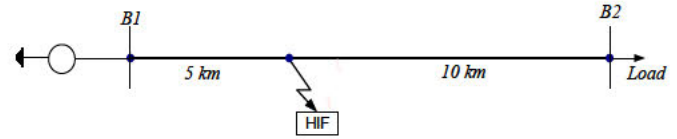


Fig. 22. Single-line diagram – HIF fault on 5th kilometer of overhead line in overall 15 km length.

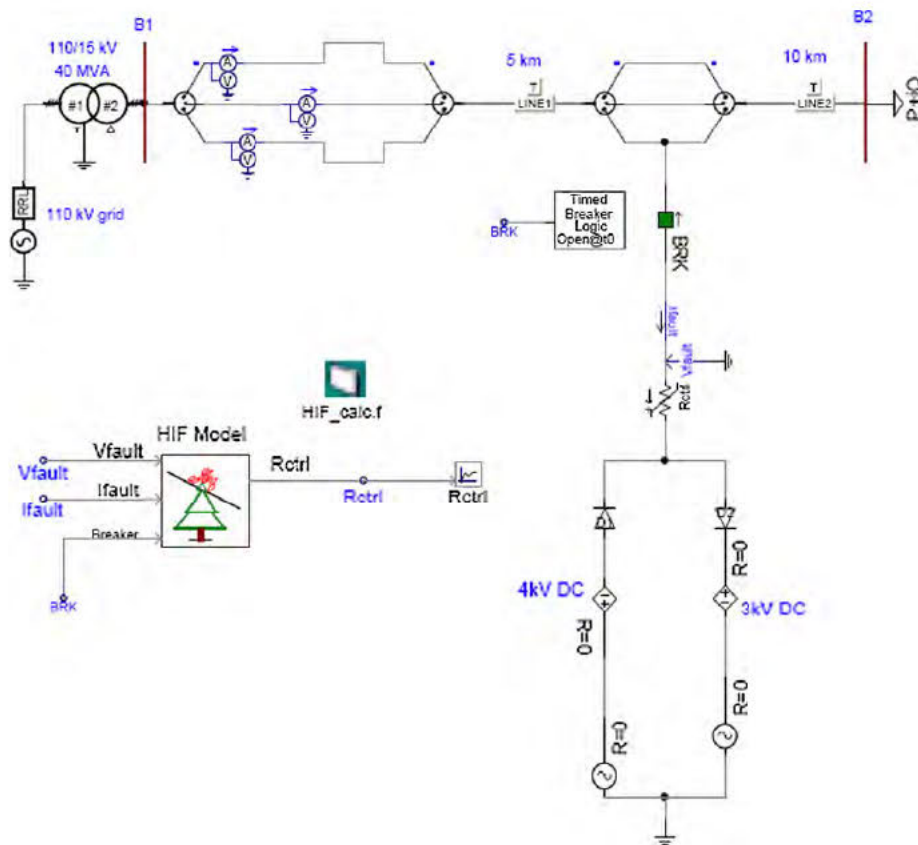


Fig. 23. Simulation setup used for determining the complex space-phasor in a case of HIF fault on 5th kilometer of overhead line in overall 15 km length.

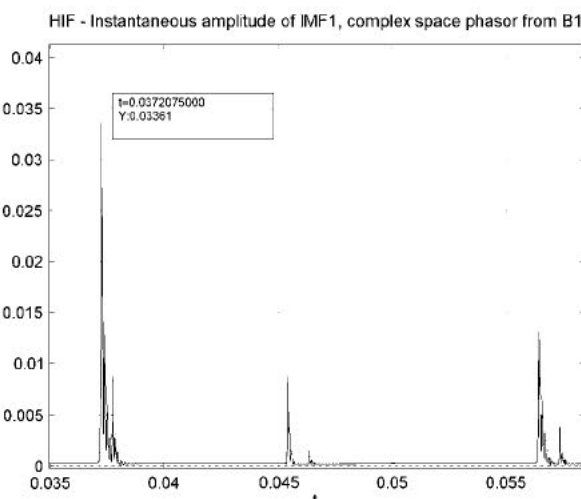


Fig. 24. Instantaneous amplitude of IMF1 component of complex space-phasor synthesized from measured voltages at B1 in HIF at 5th kilometer.

main substation, at 10 kV busbar B1. IMF1 components of fault traveling wave will be extracted by means of empirical mode decomposition (EMD) (Fig. 24).

At the moment of fault inception, singularity in complex space phasor will be detected on measuring instruments installed at main substation, at 10 kV busbar B2 (Fig. 25).

Using the speed of complex space phasor along overhead line $v = 2.9717 \times 10^8$ m/s and (9) the fault location distance at of 4899.6 m is obtained with the error of 100.3 m. Obtained error is in acceptable range regarding overall overhead line length of 15 km.

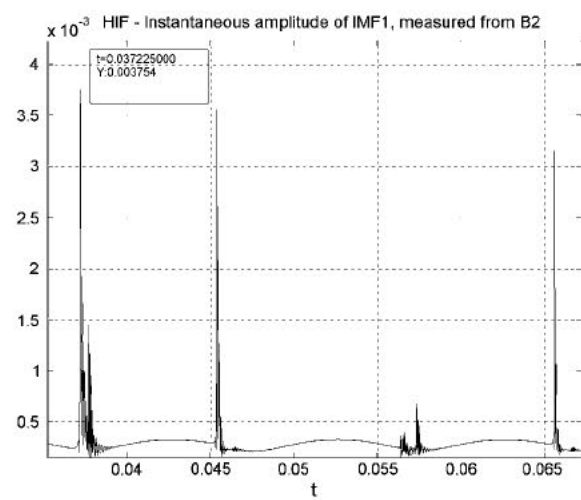


Fig. 25. Instantaneous amplitude of IMF1 component of complex space-phasor synthesized from measured voltages at B2 in HIF at 5th kilometer.

6. Conclusion

This work presents the solution of practical power grid faults location using the state of the art digital signal processing method. Complex space phasors were synthesized from measured fault voltages in typical distribution or transmission networks. Then, the Hilbert Huang transform is applied to complex space phasors in order to calculate fault locations. Obtained results have satisfactory accuracy regarding the complexity of investigated networks.

In future works we aim at decreasing the measuring frequency resolution below 2 MHz as we used in this work.

Acknowledgments

Authors thank M. Lukowicz [14] and E. Rosolowski from Wroclaw University of Technology for helpful advice on HIF modeling.

References

- [1] Serrano-Iribarregiay L. The modern space–phasor theory, part I, 1st coherent formulation and its advantages for transient analysis of converter-fed AC machines. *ETEP* 1993;3(2):171–80.
- [2] Senroy N, Suryanarayanan S, Ribeiro PF. An improved Hilbert–Huang method for analysis of time-varying waveforms in power quality. *IEEE Trans Power Syst* 2007;22(4):1843–50.
- [3] Lezama Zarraga F. On-line extraction of modal characteristics from power system measurements based on Hilbert–Huang analysis. In: 6th international conference on electrical engineering, computing science and automatic control; 2009.
- [4] Xingzhi Wang, Zheng Yan. Multiple scale identification of power system oscillations using an improved Hilbert–Huang transform. In: Power systems conference and exposition, PSCE '09; 2009.
- [5] Drummond CF, Sutanto D. Classification of power quality disturbances using the iterative Hilbert–Huang transform. In: 14th international conference on harmonics and quality of power (ICHQP); 2010. p. 1–7.
- [6] Liguo, Xu, Jian, Tianye, Yongshen. Power systems faults location with traveling wave based on Hilbert–Huang Transform. In: International conference on energy and environment technology; 2009. p. 197–200.
- [7] Zhang X, Zeng J, Li W. Traveling wave fault location of transmission line using Hilbert–Huang Transform. DRPT2008 Nanjing China; 2008.
- [8] Zhenghua Li. Hilbert–Huang transform based application in power system fault detection. In: International workshop on intelligent systems and applications, 2009. ISA; 2009. p. 1–4.
- [9] Huang Norden Eh, Shen SamuelS. Hilbert–Huang transform and its applications. World Scientific Publishing Co.; 2005.
- [10] Mansour MM, Swift GW. A multi-microprocessor based travelling wave relay – theory and realization. *IEEE Trans Power Deliv* 1986;1(1):272–9.
- [11] Kizilcay M, Pniok T. Digital simulation of fault arcs in power systems. *ETEP* 1991;1(1):55–9.
- [12] Wai DCT, Yibin X. A novel technique for high impedance fault identification. *IEEE Trans Power Deliv* July 1998;13(3):738–44.
- [13] Emanuel AE, Gulachenski EM. High impedance fault arcing on sandy soil in 15kV distribution feeders: contribution to the evaluation of the low frequency spectrum. *IEEE Trans Power Deliv* April 1990;5(2):676–86.
- [14] Michalik M, Rebizant W, Lukowicz M, Lee S-J, Kang S-H. High-impedance fault detection in distribution networks with use of wavelet-based algorithm. *IEEE Trans Power Deliv* 2006;21(4):1793–802.
- [15] [PSCAD/EMTDC] Power system simulation software manual. Manitoba HVDC Research Center; 1995.
- [16] Kim C-H, Kim H, Ko Y-H, Byun S-H, Aggarwal RK, Johns AT. A novel fault-detection technique of high-impedance arcing faults in transmission lines using the wavelet transform. *IEEE Trans Power Deliv* 2002;17(4):921–9.
- [17] Bernadić A, Leonowicz Z. Power line fault location using the complex space-phasor and Hilbert–Huang transform. 2011;R. 87(5):204–7.
- [18] Eisa Amir AA, Ramar K. Accurate one-end fault location for overhead transmission lines in interconnected power systems". *Int J Electr Power Energy Syst* 2010;32(5):383–9.
- [19] Ngu EE, Ramar K. A combined impedance and traveling wave based fault location method for multi-terminal transmission lines. *Int J Electr Power Energy Syst* 2011;33(10):1767–75.
- [20] Saha S, Aldeen M, Tan CP. Fault detection in transmission networks of power systems. *Int J Electr Power Energy Syst* 2011;33(4):887–900.
- [21] Li Zewen, Yao Jiangang, Zeng Xiangjun, Deng Feng. Power grid fault traveling wave network protection scheme. *Int J Electr Power Energy Syst* 2011;33(4):875–9.